

Boosting Knowledge Graph Foundation Models via Enhanced Negative Sampling

Yinan Liu
Northeastern University
Shenyang, China
liuyinan@cse.neu.edu.cn

Wenjin Xu
Northeastern University
Shenyang, China
xuwenjin@mails.neu.edu.cn

Zhiyuan Zha
Northeastern University
Shenyang, China
chazy@mails.neu.edu.cn

Xiaochun Yang*
Northeastern University
Shenyang, China
yangxc@mail.neu.edu.cn

Bin Wang
Northeastern University
Shenyang, China
binwang@mail.neu.edu.cn

Abstract

Knowledge graphs (KGs) have become the core backbone of numerous downstream tasks such as question answering and recommender systems. However, despite all this, KGs are often very incomplete. To perform zero-shot knowledge graph completion in unseen KGs, which have different relational vocabularies from those used for pre-training, KG foundation models (KGfMs) receive a wide range of attention. Existing KGfMs often perform training using random negative triples, which are constructed by replacing the head or tail entity of a positive triple with a random entity. However, these negative triples are often constructed with limited quality, providing weak supervision for KGfM training. In this paper, we propose a simple yet effective adaptive negative sampling approach, KMAS, to enhance existing KGfMs. KMAS constructs hard negative triples through the updated relation embeddings generated from the existing KGfM’s relation encoder. To further adaptively align with the evolving capability of the KGfM during the training process, KMAS adjusts the ratio of hard negative triples dynamically throughout the whole training process: after a warmup phrase, it increases the ratio linearly and then decreases linearly. Extensive experiments are conducted over 44 data sets. Experimental results demonstrate that our proposed negative sampling method can enhance many SOTA KGfMs without requiring excessive additional time or memory consumption.

Keywords

Knowledge Graph Foundation Model, Negative Sampling

1 Introduction

Knowledge graphs (KGs), which consist of massive amounts of knowledge in the form of triples (head entity, relation, tail entity), have become the core backbone of numerous downstream tasks such as question answering [28] and recommender systems [23]. However, despite all this, KGs are often very incomplete [12], making the task of link prediction [13, 14] increasingly important. Traditional transductive link prediction methods (e.g., TransE [3] and RotatE [17]) learn entity/relation embeddings constrained by specific entity and relation vocabularies, lacking the ability to generalize to unseen entities/relations on KGs. To address the limitation, partially inductive link prediction approaches [11] relax the constraint on

entities and generalize to unseen entities while keeping the relation vocabulary fixed. Fully inductive link prediction approaches [9] further relax the constraint on relations and generalize to both unseen entities and unseen relations, which motivates the development of knowledge graph foundation models (KGfMs). KGfMs learn invariance of the relation structure [5] by pre-training on multiple KGs of different entity/relation vocabularies, thereby enabling zero-shot reasoning on unseen KGs.

Existing KGfMs (e.g., ULTRA [5], TRIX [27], MOTIF [7], and SEMMA [1]) usually adopt a common procedure: (1) construct a relation graph based on the KG; (2) apply a relation encoder on this relation graph to obtain relation embeddings; (3) use the obtained relation embeddings and employ an entity encoder on the KG to obtain final link prediction results. It is worth noting that the training process of these KGfMs’ relation and entity encoders is based on random negative triples, which are constructed by replacing the head or tail entity of a positive triple with a random entity. Although straightforward and efficient, these negative triples are often constructed with limited quality (i.e., “easy negative triples”), providing weak supervision. Since these easy negative triples do not be dynamically adjusted throughout the whole training process, they fail to align with the KGfM’s evolving capabilities. For instance, given a positive triple (*Obama, born_in, Hawaii*), a randomly constructed negative triple like (*Obama, born_in, Basketball*) is trivial for a well-trained KGfM. Conversely, constructing “hard negative triples” such as (*Obama, born_in, Chicago*)—which is factually incorrect yet semantically plausible—can provide more challenging training samples to enhance the learned embeddings, improving the generalization ability of the KGfM.

In this paper, to enhance existing KGfMs, we propose a simple yet effective adaptive negative sampling method KMAS. To construct hard negative triples for improving the training process of the KGfM, KMAS leverages the relation embeddings generated by the relation encoder of an existing KGfM to construct the tail (head) entity distribution, which enables hybrid negative sampling. In order to adaptively align with the evolving capability of the KGfM during the training process, KMAS iteratively updates relation embeddings using the encoder from the last training iteration. This update refines the tail (head) entity distribution and thereby generates progressively more effective negative samples. Notably, KMAS dynamically adjusts the ratio of hard negative triples throughout

*Corresponding author

the training process: after a warmup phase that employs pure random negative sampling (as in existing KGFM’s), it linearly increases the ratio of hard negative triples to a peak, then linearly decreases it in subsequent iterations.

The main contributions of this paper are summarized as follows:

- To the best of our knowledge, we are the first to enhance the negative sampling method in KGFM’s, boosting the existing KGFM’s performance.
- We propose a simple yet effective negative sampling method by adaptively constructing hard negative samples with a dynamic hard negative ratio adjustment strategy, which is flexible to adapt to many KGFM’s.
- We conduct extensive experiments on 44 data sets. Experimental results demonstrate that our proposed negative sampling method can improve the performance of many SOTA KGFM’s without requiring excessive additional time or memory consumption.

2 Preliminaries

A knowledge graph (KG) is denoted by $\mathcal{G} = (\mathcal{V}, \mathcal{R}, \mathcal{T})$, where \mathcal{V} denotes a set of entities, \mathcal{R} denotes a set of relations, and $\mathcal{T} \subseteq \mathcal{V} \times \mathcal{R} \times \mathcal{V}$ denotes a set of triples. A triple $(h, r, t) \in \mathcal{T}$ connects the head entity $h \in \mathcal{V}$ with the tail entity $t \in \mathcal{V}$ through the relation $r \in \mathcal{R}$. Given a KG $\mathcal{G} = (\mathcal{V}, \mathcal{R}, \mathcal{T})$, the corresponding relation graph $\mathcal{G}_{\mathcal{R}} = (\mathcal{V}_{\mathcal{R}}, \mathcal{E}_{\mathcal{R}})$ is a directed graph where nodes $\mathcal{V}_{\mathcal{R}}$ represent the relations \mathcal{R} . The edges $\mathcal{E}_{\mathcal{R}}$ capture interactions between relations based on their connectivity in \mathcal{T} .

Given a knowledge graph $\mathcal{G} = (\mathcal{V}, \mathcal{R}, \mathcal{T})$, the task of link prediction aims to infer missing facts based on observed ones. Formally, given a query $(h, r, ?)$ (resp. $(?, r, t)$), the goal is to predict the missing tail entity $t \in \mathcal{V}$ (resp. head entity $h \in \mathcal{V}$). During inference, for a query $(h, r, ?)$, we calculate scores for all candidate entities $t' \in \mathcal{V}$ and rank them in descending order. The objective is to rank the ground-truth entity higher than other candidates. We denote $\mathcal{G}_{train} = (\mathcal{V}_{train}, \mathcal{R}_{train}, \mathcal{T}_{train})$ as the training graph and $\mathcal{G}_{test} = (\mathcal{V}_{test}, \mathcal{R}_{test}, \mathcal{T}_{test})$ as the inference graph. We consider three generalization settings based on the overlap between \mathcal{G}_{train} and \mathcal{G}_{test} :

- Transductive setting: The entity and relation sets are shared by the training and inference processes, i.e., $\mathcal{V}_{train} = \mathcal{V}_{test}$, $\mathcal{R}_{train} = \mathcal{R}_{test}$, and $\mathcal{T}_{train} = \mathcal{T}_{test}$.
- Partially inductive setting (unseen entities): Entities at inference time are unseen during training, while the relation set is shared by the training and inference processes, i.e., $\mathcal{V}_{train} \cap \mathcal{V}_{test} = \emptyset$, $\mathcal{R}_{train} = \mathcal{R}_{test}$, and $\mathcal{T}_{train} \neq \mathcal{T}_{test}$.
- Fully inductive setting (unseen entities & relations): The most challenging foundation model setting, where both entities and relations at inference time are unseen during training, i.e., $\mathcal{V}_{train} \cap \mathcal{V}_{test} = \emptyset$, $\mathcal{R}_{train} \cap \mathcal{R}_{test} = \emptyset$, and $\mathcal{T}_{train} \neq \mathcal{T}_{test}$.

For existing KGFM’s, we use $\text{Encoder}_{\theta_r}$ to denote the relation encoder that generates relation embeddings. $\text{Encoder}_{\theta_e}$ denote the entity encoder that generates entity embeddings. f_{ω} denotes an MLP that maps these entity embeddings to final scores. θ_r denotes the parameters of the GNN architecture of $\text{Encoder}_{\theta_r}$. θ_e denotes the parameters of the GNN architecture of $\text{Encoder}_{\theta_e}$. ω denotes

the parameters of the MLP that generates the final scores. For KGFM’s, the GNN architecture often adopts NBFNet [29]. In KFGM’s, a labeling trick is used to initialize relations to generate conditional relation embeddings based on the relation graph $\mathcal{G}_{\mathcal{R}}$, which means that r of the given query (i.e., $(h, r, ?)$ or $(?, r, t)$) is initialized as an all-one vector, while other relations are initialized as all-zero vectors. $\text{Encoder}_{\theta_r}$ uses initialized relation embeddings to generate conditional relation embeddings for $\text{Encoder}_{\theta_e}$. In $\text{Encoder}_{\theta_e}$, the entity in query is initialized as the conditional relation embedding of r , and other entities are initialized as all-zero vectors. Then, $\text{Encoder}_{\theta_e}$ uses the initialized entity embeddings and conditional relation embeddings to generate entity embeddings for f_{ω} to obtain the scores, which are used to predict the missing entity in the given query.

3 The Method KMAS

3.1 Overview

In this section, we briefly introduce our proposed method KMAS. Specifically, during each iteration of an existing KGFM’s training process, KMAS first calculates relation similarities to identify the relations that are semantically similar to the target relation of each positive triple based on the relation embeddings generated through $\text{Encoder}_{\theta_r}$ based on the relation graph (Section 3.2). Next, using these similarities, KMAS assigns weights to entities to construct head (tail) entity distributions for hard negative sample generation (Section 3.3). Then, a hybrid sampling strategy is employed to construct the final negative triple set for each triple by combining random and hard negative samples according to different distributions (Section 3.4). Furthermore, KMAS dynamically adjusts the ratio of hard negative samples versus random negative samples throughout training iterations, which follows a trade-off policy by combining both “easier first” as curriculum learning and “harder first” as hard example mining: beginning with a warmup phase without hard negative samples, increasing linearly to a peak, and then decreasing linearly (Section 3.5). Thus, the KGFM’s $\text{Encoder}_{\theta_r}$ can be trained based on the training set consisting of positive triples and adaptively constructed negative triples (Section 3.6). After multiple iterations, the relation embeddings generated from $\text{Encoder}_{\theta_r}$, together with the KGFM’s entity encoder Encoder_e and f_{ω} , are utilized to score all candidates for each test triple (Section 3.6).

3.2 Relation Similarity Acquisition

To construct high-quality hard negative samples for positive triples, we first utilize the relation embeddings generated by $\text{Encoder}_{\theta_r}$ to measure the similarities between the relations. For the relation r of a given positive triple (h, r, t) , we input it into $\text{Encoder}_{\theta_r}$ to obtain relation embeddings for all relations in \mathcal{G} as follows:

$$H \leftarrow \text{Encoder}_{\theta_r}(\mathcal{G}_{\mathcal{R}}, r, t), \quad (1)$$

where d denotes the dimension of embeddings in $\text{Encoder}_{\theta_r}$, $H \in \mathbb{R}^{|\mathcal{R}| \times d}$ denotes the set of relation embeddings. If SEMMA’s relation encoder is selected as $\text{Encoder}_{\theta_r}$, t is set to the text of relations. For other KGFM’s (i.e., ULTRA, TRIX, and MOTIF), t is set to none. Then, based on H , we can calculate the similarity vector $\mathbf{S} \in \mathbb{R}^{|\mathcal{R}|}$ between r and the relation r_o in \mathcal{R} as follows:

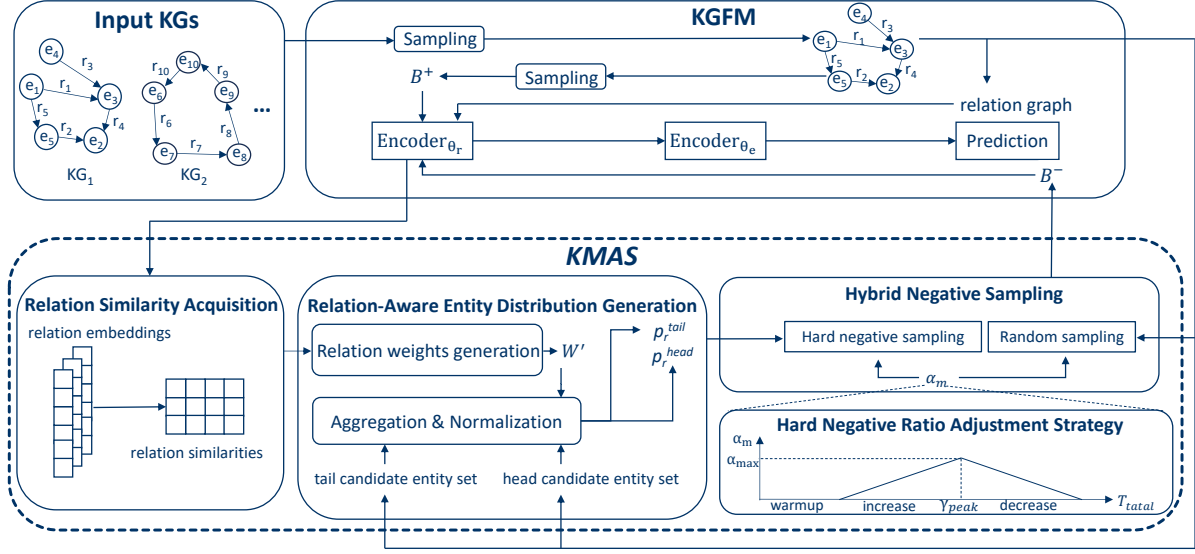


Figure 1: The overall training process of our proposed negative sampling method KMAS.

$$S(r, r_o) = \text{Sim}(\mathbf{h}_r, \mathbf{h}_{r_o}) \quad (2)$$

where the function $\text{Sim}(\cdot)$ is implemented by the cosine similarity, \mathbf{h}_r denotes the relation embedding of r and \mathbf{h}_{r_o} denotes the relation embedding of r_o . Specifically, we set $S(r, r)$ to $-\infty$, which will prevent the relation itself from sampling in the following process. Based on this, we construct the vector $W_r \in \mathbb{R}^{|\mathcal{R}|}$ for r to store relation similarities using the Softmax function with a temperature coefficient τ as follows:

$$W_{r,j} = \frac{\exp(S_{r,j}/\tau)}{\sum_{j'=1}^{|\mathcal{R}|} \exp(S_{r,j'}/\tau)}, j = 1, 2, \dots, |\mathcal{R}|. \quad (3)$$

3.3 Relation-Aware Entity Distribution Generation

First, we sort the weights of relations in W_r in descending order to obtain W_r^* . Next, for r , we select the top K relations $R_{\text{top}K}(r)$ whose sum of weights exceeds a threshold q as follows:

$$K = \arg \min_z z, \quad \text{s.t.} \quad \sum_{y=1}^z W_{r,y}^* \geq q, \quad z \in \{1, \dots, |\mathcal{R}|\}. \quad (4)$$

For the relations not in $R_{\text{top}K}(r)$, we set their weights to zero. Subsequently, we reweight the selected relations to construct a weight matrix W' by calculating the weight $W'_{r,b}$ for every relation r and its corresponding selected relation b as follows:

$$W'_{r,b} = \frac{W_{r,b}^*}{\sum_{b'=1}^K W_{r,b'}^*}, b = 1, 2, \dots, K. \quad (5)$$

To generate hard negative samples for the given positive triple (h, r, t) , we construct the sets of candidate entities w_r^{tail} (resp. w_r^{head}) by searching entities in \mathcal{V} that can act as tail (resp. head) entities of the selected relations from $R_{\text{top}K}(r)$ in \mathcal{G} . Thus, we can obtain

the weight $x_{r,e}^{\text{tail}}$ of an entity e as the tail entity of r by aggregating the relation weights as follows:

$$x_{r,e}^{\text{tail}} = \sum_{r' \in R_{\text{top}K}(r)} W'_{r,r'} \cdot I_{\text{tail}}(r', e). \quad (6)$$

$$I_{\text{tail}}(r', e) = \begin{cases} 1 & \text{if } e \in w_{r'}^{\text{tail}} \text{ and } r' \in R_{\text{top}K}(r), \\ 0 & \text{otherwise.} \end{cases} \quad (7)$$

It can be seen that if an entity frequently appears as the tail entity of the relation that is similar to r , this entity will be assigned a high probability score. Then, we normalize these weights of entities to obtain a tail entity probability distribution $\mathcal{P}_r^{\text{tail}}$ for r as follows:

$$\mathcal{P}_r^{\text{tail}}(e) = \frac{x_{r,e}^{\text{tail}}}{\sum_{e' \in \mathcal{V}} x_{r,e'}^{\text{tail}}}. \quad (8)$$

Note that, we can obtain the weight $x_{r,e}^{\text{head}}$ of an entity e as the head entity of r and the head entity probability distribution $\mathcal{P}_r^{\text{head}}$ for r in a similar way, which is omitted due to the length of the paper.

3.4 Hybrid Negative Sampling

To improve the model's performance, we propose a hybrid sampling strategy to provide more challenging negative samples while still retaining the simpler samples, preserving the fundamental ability to distinguish between positive and negative samples. We denote \mathcal{B}^+ as a batch of positive triples. For each positive triple (h, r, t) in \mathcal{B}^+ , we construct its corresponding negative sample set $\mathcal{B}_{(h,r,t)}^-$. Specifically, for (h, r, t) , we draw N_{rand} entities randomly from \mathcal{V} to obtain $\mathcal{T}_{(h,r,t)}^{\text{rand}}$ (resp. $\mathcal{H}_{(h,r,t)}^{\text{rand}}$), and draw the N_{hard} entities according to the distribution $\mathcal{P}_r^{\text{tail}}$ (resp. $\mathcal{P}_r^{\text{head}}$) to obtain $\mathcal{T}_{(h,r,t)}^{\text{hard}}$ (resp. $\mathcal{H}_{(h,r,t)}^{\text{hard}}$). The number of random negative samples N_{rand} and hard negative samples N_{hard} are calculated as follows:

$$N_{\text{rand}} = \lfloor N \cdot (1 - \alpha_m) \rfloor, \quad (9)$$

$$N_{hard} = N - N_{rand}. \quad (10)$$

Note that α_m denotes the current hard negative ratio, which will be calculated in Section 3.5. The negative sample sets $\mathcal{C}_{(h,r,t)}^{tail}$ and $\mathcal{C}_{(h,r,t)}^{head}$ are constructed as follows:

$$\mathcal{C}_{(h,r,t)}^{tail} = \{(h, r, t') | t' \in \mathcal{T}_{(h,r,t)}^{rand} \cup \mathcal{T}_{(h,r,t)}^{hard}\}, \quad (11)$$

$$\mathcal{C}_{(h,r,t)}^{head} = \{(h', r, t) | h' \in \mathcal{H}_{(h,r,t)}^{rand} \cup \mathcal{H}_{(h,r,t)}^{hard}\}. \quad (12)$$

Based on these, we can construct the final negative sample set $\mathcal{B}_{(h,r,t)}^-$ for (h, r, t) as follows:

$$\mathcal{B}_{(h,r,t)}^- = \begin{cases} \mathcal{C}_{(h,r,t)}^{tail} & \text{if } (h, r, t) \text{ is in the first half of } \mathcal{B}^+, \\ \mathcal{C}_{(h,r,t)}^{head} & \text{otherwise.} \end{cases} \quad (13)$$

Thus, by constructing negative samples for each positive triple in \mathcal{B}^+ according to the above procedure, we can obtain the corresponding negative sample set \mathcal{B}^- of \mathcal{B}^+ .

3.5 Hard Negative Ratio Adjustment Strategy

Inspired by the previous study [22], which combines both "easier first" as curriculum learning and "harder first" as hard example mining, we propose a strategy for hard negative sampling to dynamically adjust the ratio between random negative samples and our constructed hard negative samples. We define the hard negative ratio α_m as a piecewise linear function, which is controlled by the warmup ratio β_{warm} ranging from 0 to 1, the peak position γ_{peak} , and the maximum ratio of the hard negative samples α_{max} . Crucially, γ_{peak} determines the point where α_m reaches its maximum value α_{max} within the remaining training process after the warmup phase, which means γ_{peak} is greater than β_{warm} and less than 1. Let m denote the m -th iteration of the whole training iterations and T_{total} denote the total number of training iterations. We calculate the ratio of completed iterations p_m as follows:

$$p_m = \frac{m}{T_{total}}. \quad (14)$$

We can calculate α_m for the current m -th iteration based on the following rules.

- If p_m is less than β_{warm} , we set α_m to 0.
- If p_m is greater than or equal to β_{warm} and less than P_{peak} , α_m is calculated as follows:

$$\alpha_m = \alpha_{max} \cdot \frac{p_m - \beta_{warm}}{P_{peak} - \beta_{warm}}. \quad (15)$$

- If p_m is greater than or equal to P_{peak} , α_m is calculated as follows:

$$\alpha_m = \alpha_{max} \cdot \frac{1 - p_m}{1 - P_{peak}}, \quad (16)$$

where P_{peak} equals $\beta_{warm} + \gamma_{peak}(1 - \beta_{warm})$.

For the hard negative ratio during the whole training process, this heuristic adjustment strategy is simple yet effective, which is verified by our experiments (Section 4.5).

3.6 Training

The KGFM is often trained by minimizing the binary cross-entropy loss function. We obtain the prediction score $s(h, r, t)$ of a triple (h, r, t) via f_ω . The optimization objective for a given positive triple (h, r, t) and its corresponding negative triple set $\mathcal{B}_{(h,r,t)}^-$ is defined as follows:

$$\mathcal{L}(h, r, t) = -\log(\sigma(s(h, r, t))) - \sum_{(h', r, t') \in \mathcal{B}_{(h,r,t)}^-} w(h', r, t') \log(1 - \sigma(s(h', r, t'))), \quad (17)$$

where σ is the Sigmoid activation function. Additionally, considering that different negative samples have different importance to the training process of the KGFM, we assign the normalized weight to each negative sample using the Softmax function with a temperature coefficient τ_{adv} as follows:

$$w(h', r, t') = \frac{\exp(s(h', r, t')/\tau_{adv})}{\sum_{(h_k, r, t_k) \in \mathcal{B}_{(h,r,t)}^-} \exp(s(h_k, r, t_k)/\tau_{adv})}. \quad (18)$$

Finally, the total optimization objective for the given batch \mathcal{B}^+ is calculated by averaging the losses over all positive triples in \mathcal{B}^+ as follows:

$$\mathcal{L}_{total} = \frac{1}{|\mathcal{B}^+|} \sum_{(h,r,t) \in \mathcal{B}^+} \mathcal{L}(h, r, t). \quad (19)$$

It is worth mentioning that the processes of the relation similarity acquisition (Section 3.2) and the relation-aware entity distribution generation (Section 3.3) are fully adaptive. Since the parameters of the relation encoder θ_r are updated continuously through the backpropagation mechanism during the training process of the KGFM, the embeddings of the relations also evolve throughout the whole training process. Consequently, even for the same KG and the same relation sampled in different iterations, the values of weights W_r and the tail (resp. head) entity distribution \mathcal{P}_r^{tail} (resp. \mathcal{P}_r^{head}) also change dynamically for each iteration. This mechanism ensures that the constructed negative samples are time-variant. Although these negative samples may not be the most difficult, they represent the most challenging negative samples for the current state of the KGFM. The details of the training process are shown in Algorithm 1. Additionally, we adopt the same inference procedure as previous KGFM studies [1, 5, 7, 27].

3.7 Complexity Analysis

Here, we analyze the time and memory complexity of KMAS. $|\mathcal{V}|$ and $|\mathcal{R}|$ denote the numbers of entities and relations, respectively. $|\mathcal{T}|$ denotes the number of triples in the KG. L denotes the number of GNN layers. $|\mathcal{B}^+|$ denotes the batch size. \bar{d}_{rel} denotes the average relation degree.

The time complexity of KMAS is analyzed as follows. The time complexity of the relation similarity acquisition (Section 3.2) is $\mathcal{O}(|\mathcal{B}^+| \cdot |\mathcal{R}| \cdot d)$ (line 13 - 14 in Algorithm 1). The time complexity of the relation-aware entity distribution generation (Section 3.3) is $\mathcal{O}(|\mathcal{B}^+| \cdot (|\mathcal{R}|(\log |\mathcal{R}| + \bar{d}_{rel}) + |\mathcal{V}|))$ (line 15 - 18 in Algorithm 1). The time complexity of the hybrid sampling strategy (Section 3.4) is $\mathcal{O}(|\mathcal{B}^+| \cdot N)$ (line 19 - 25 in Algorithm 1). Consequently,

Algorithm 1: KMAS

```

1 Input: KGs  $\mathcal{G}_1, \mathcal{G}_2, \dots, \mathcal{G}_n$ , relation graphs  $\mathcal{G}_{R_1}, \mathcal{G}_{R_2}, \dots, \mathcal{G}_{R_n}$ ,
   the entity encoder  $\text{Encoder}_{\theta_e}$ , the relation encoder
    $\text{Encoder}_{\theta_r}$ , the MLP  $f_\omega$ , the number of negatives  $N$ ,
   threshold  $q$ , temperatures  $\tau$  and  $\tau_{adv}$ , total number of
   iterations  $T_{\text{total}}$ , warmup ratio  $\beta_{\text{warm}}$ , peak position  $\gamma_{\text{peak}}$ ,
   maximum ratio of the hard negative samples  $\alpha_{\text{max}}$ 
2 Output: Optimized parameters  $\theta_r, \theta_e$  and  $\omega$ 
3 Initialize  $\theta_r, \theta_e$ , and  $\omega$  randomly
4 for  $m = 1$  to  $T_{\text{total}}$  do
5     Randomly sample a KG  $\mathcal{G}_i$  and a batch of positive triples
        $\mathcal{B}^+$  from  $\mathcal{G}_i$ 
6     Calculate the ratio of completed iterations  $p_m$  via
       Formula (14)
7     for each positive triple  $(h, r, t) \in \mathcal{B}^+$  do
8         if  $p_m < \beta_{\text{warm}}$  then
9              $\alpha_m \leftarrow 0$ 
10            Draw  $N_{\text{rand}}$  entities from  $\mathcal{V}$  randomly
11            Construct the negative sample set  $\mathcal{B}_{(h,r,t)}^-$  for
                $(h, r, t)$  by replacing the head/tail entity with a
               random entity in  $\mathcal{G}_i$ 
12        else
13             $H \leftarrow \text{Encoder}_{\theta_r}(\mathcal{G}_{R_i}, r, t)$ 
14            Calculate the weight vector  $W_r$  via Formula (3)
15            Generate the relation set  $R_{\text{top}K}(r)$  based on  $W_r$ 
16            Calculate  $W'$  via Formula (5)
17            Calculate the weights of entities  $x_{r,e}^{\text{tail}}$  and  $x_{r,e}^{\text{head}}$ 
               via Formula (6) based on  $W'$  and  $R_{\text{top}K}(r)$ 
18            Generate entity probability distributions  $\mathcal{P}_r^{\text{tail}}$ 
               and  $\mathcal{P}_r^{\text{head}}$  via Formula (8)
19            if  $p_m < P_{\text{peak}}$  then
20                Update  $\alpha_m$  via Formula (15)
21            else
22                Update  $\alpha_m$  via Formula (16)
23            Draw  $N_{\text{rand}}$  entities from  $\mathcal{V}$  randomly
24            Draw  $N - N_{\text{rand}}$  entities according to  $\mathcal{P}_r^{\text{tail}}$  and
                $\mathcal{P}_r^{\text{head}}$ 
25            Construct the negative sample set  $\mathcal{B}_{(h,r,t)}^-$  for
                $(h, r, t)$  via Formula (13)
26        Calculate the loss via Formula (19) based on  $\mathcal{B}^+$  and its
           corresponding negative triple set
           
$$\mathcal{B}^- = \bigcup_{(h,r,t) \in \mathcal{B}^+} \mathcal{B}_{(h,r,t)}^-$$

27        Update  $\theta_r, \theta_e$ , and  $\omega$ 

```

the total time complexity for training is $O(T_{\text{total}} \cdot |\mathcal{B}^+| \cdot (|\mathcal{R}|(d + \log |\mathcal{R}| + \bar{d}_{\text{rel}}) + |\mathcal{V}| + N))$. Considering $|\mathcal{R}|$ is usually small and $|\mathcal{B}^+|/\bar{d}_{\text{rel}}/T_{\text{total}}/N$ is a constant, therefore the time complexity of KMAS is linear to $|\mathcal{V}|$. The time complexity of the existing base KGFM is dominated by $|\mathcal{T}|$. Compared with $|\mathcal{T}|$, $|\mathcal{V}|$ is small, indicating a marginal overhead generated by KMAS, which is verified in Section 4.3.

The memory complexity of KMAS is analyzed as follows. The memory complexity of the relation similarity acquisition (Section 3.2) is $O(|\mathcal{B}^+| \cdot |\mathcal{R}|)$ (line 13 - 14 in Algorithm 1). The memory complexity of the relation-aware entity distribution generation (Section 3.3) is $O(|\mathcal{B}^+| \cdot |\mathcal{V}|)$ (line 15 - 18 in Algorithm 1). The memory complexity of the hybrid negative sampling (Section 3.4) is $O(|\mathcal{B}^+| \cdot N)$ (line 19 - 25 in Algorithm 1). Consequently, the total memory complexity of our method is $O(|\mathcal{B}^+|(|\mathcal{R}| + |\mathcal{V}| + N))$. Considering $|\mathcal{R}|$ is usually small and N is a constant, therefore the memory complexity of KMAS is linear to $|\mathcal{B}^+| \cdot |\mathcal{V}|$. The base KGFM need to store intermediate node embeddings across all L layers to compute gradients during backpropagation, with a memory complexity of $O(|\mathcal{B}^+| \cdot |\mathcal{V}| \cdot d \cdot L)$. Compared with $|\mathcal{B}^+| \cdot |\mathcal{V}| \cdot d \cdot L$, $|\mathcal{B}^+| \cdot |\mathcal{V}|$ is small, indicating a marginal overhead generated by KMAS, which is verified in Section 4.4.

4 Experiments

4.1 Experimental Setting

4.1.1 Data Sets. We utilize a unified pre-training corpus containing 3 common KGs to train KGFM: FB15k-237 [19], WN18RR [4], and CoDEx-Medium [15]. This combination covers general-world knowledge and diverse Wikipedia domains, enabling the KGFM to learn general structural patterns. We perform extensive experiments on 44 data sets that are categorized into transductive, partially inductive, and fully inductive settings to evaluate the generalizability of our proposed method. The definitions of these settings have been introduced in Section 2. More detailed information of the data sets used in our experiments can be found in Appendix A.

4.1.2 Evaluation Metrics. We adopt the same evaluation metrics, mean reciprocal rank (MRR) and Hits@10, as previous KGFM studies [1, 5, 7, 27] to evaluate the performance of KGFM and KGFM using KMAS as the negative sampling method. Both metrics are reported under the filtered ranking protocol [3].

4.1.3 Base KGFM. To demonstrate the effectiveness of KMAS, we perform KMAS on many SOTA KGFM (i.e., ULTRA, TRIX, MOTIF, and SEMMA), which are introduced in detail as follows.

ULTRA [5] constructs the relation graph, where nodes denote relations in the KG and edges denote four fundamental interactions between relations in the KG: $h2h, t2t, h2t$, and $t2h$. An edge between relation r_i and r_j is established in $\mathcal{G}_{\mathcal{R}}$ if there exist triples (h_i, r_i, t_i) and $(h_j, r_j, t_j) \in \mathcal{T}$ satisfying one of the following conditions: (1) $h2h: h_i = h_j$; (2) $t2t: t_i = t_j$; (3) $h2t: h_i = t_j$; (4) $t2h: t_i = h_j$. Specifically, the four fundamental interactions are learnable embeddings, which form part of θ_r . $\text{Encoder}_{\theta_r}$ works on the relation graph to generate relation embeddings. $\text{Encoder}_{\theta_e}$ uses these relation embeddings to generate entity embeddings for f_ω to predict entities.

TRIX [27] constructs four relation graphs, where nodes denote relations in the KG and edges denote specific entities that bridge two relations through one of four fundamental interactions: $h2h, t2t, h2t$, and $t2h$. $\text{Encoder}_{\theta_r}$ of TRIX captures relation interactions through this entity-aware edge information. $\text{Encoder}_{\theta_e}$ and f_ω of TRIX adopt the same mechanism as ULTRA. Specially, TRIX adopts an iterative architecture, stacking modules in the sequence: $\text{Encoder}_{\theta_{r_1}} \rightarrow \text{Encoder}_{\theta_{e_1}} \rightarrow \text{Encoder}_{\theta_{r_2}} \rightarrow \text{Encoder}_{\theta_{e_2}} \rightarrow \dots \rightarrow \text{Encoder}_{\theta_{r_n}} \rightarrow \text{Encoder}_{\theta_{e_n}}$. Note that $\text{Encoder}_{\theta_{r_1}}, \text{Encoder}_{\theta_{r_2}}, \dots$,

Table 1: Performance on the task of link prediction under different settings (i.e., inductive (e, r), inductive (e), transductive) over 44 data sets. Since SCR’s source codes are not publicly available, we obtain the results of SCR from [20]. The performance of other KGfMs (i.e., ULTRA, TRIX, MOTIF, and SEMMA) is reproduced via their open-source solutions.

Model	Inductive (e, r) (19 graphs)		Inductive (e) (16 graphs)		Transductive (9 graphs)		Total Avg (44 graphs)	
	MRR	Hits@10	MRR	Hits@10	MRR	Hits@10	MRR	Hits@10
SCR (NIPS’25) [20]	0.320	0.498	0.435	0.592	0.298	0.447	0.358	0.523
ULTRA (ICLR’24) [5]	0.317	0.499	0.429	0.578	0.331	0.483	0.360	0.524
ULTRA + KMAS	0.326	0.508	0.434	0.584	0.337	0.490	0.367	0.532
TRIX (LoG’24) [27]	0.337	0.523	0.445	0.601	0.304	0.467	0.370	0.540
TRIX + KMAS	0.340	0.523	0.454	0.601	0.307	0.471	0.375	0.541
MOTIF (ICML’25) [7]	0.329	0.498	0.433	0.582	0.324	0.477	0.360	0.516
MOTIF + KMAS	0.333	0.508	0.437	0.588	0.333	0.486	0.365	0.524
SEMMA (EMNLP’25) [1]	0.331	0.502	0.447	0.590	0.327	0.479	0.372	0.529
SEMMA + KMAS	0.341	0.517	0.451	0.593	0.336	0.487	0.380	0.539

Encoder $_{\theta_{rn}}$ work on the same four relation graphs and Encoder $_{\theta_{e_1}}$, Encoder $_{\theta_{e_2}}, \dots, \text{Encoder}_{\theta_{e_n}}$ work on the same KG.

MOTIF [7] constructs the relation hypergraph, where hyperedges are matches of arbitrary graph motifs (i.e., 2-path and 3-path motifs) from the KG, and nodes are relations in the KG. Encoder $_{\theta_r}$ of MOTIF works on the hypergraph, and the arbitrary graph motifs are the learnable embeddings that are part of θ_r for Encoder $_{\theta_r}$. Encoder $_{\theta_e}$ and f_{ω} of MOTIF adopt the same mechanism as ULTRA.

SEMMA [1] constructs a structural relation graph and a textual relation graph. For the textual relation graph, nodes denote relations, and weighted edges between them denote the cosine similarity of their textual embeddings. Encoder $_{\theta_r}$ of SEMMA works on the two relation graphs in parallel and uses an MLP to integrate their information and obtain the final relation embeddings. Encoder $_{\theta_e}$ and f_{ω} of SEMMA adopt the same mechanism as ULTRA.

4.1.4 Implementation Details. We adopt the official implementation of 4 KGfMs (i.e. ULTRA, TRIX, MOTIF, and SEMMA) as base KGfMs. Hyperparameters N , q , τ , τ_{adv} , β_{warm} , γ_{peak} , and α_{max} are set to 512, 0.4, 0.8, 1, 0.25, 0.25 and 0.4 for all KGfMs with KMAS as the negative sampling method, respectively. T_{total} is set to 800000 for ULTRA and SEMMA and 10000 for TRIX and MOTIF. All experiments are conducted on NVIDIA 4080 GPUs with the same version of PyTorch and PyG. We make the data sets and source code available for future research¹.

4.2 Effectiveness Study

We utilize Encoder $_{\theta_r}$ to generate relation embeddings for the construction of hard negative samples in ULTRA, TRIX, MOTIF, and SEMMA. Specifically, for TRIX, we use Encoder $_{\theta_{r_1}}$ to generate relation embeddings to construct hard negative samples. Additionally, for SCR, the relation graph is enhanced by deriving both global and query-aware relation embeddings and injecting them to guide semantic-conditioned message passing on the KG. Note that SCR does not open-source their code, so we show the results from the

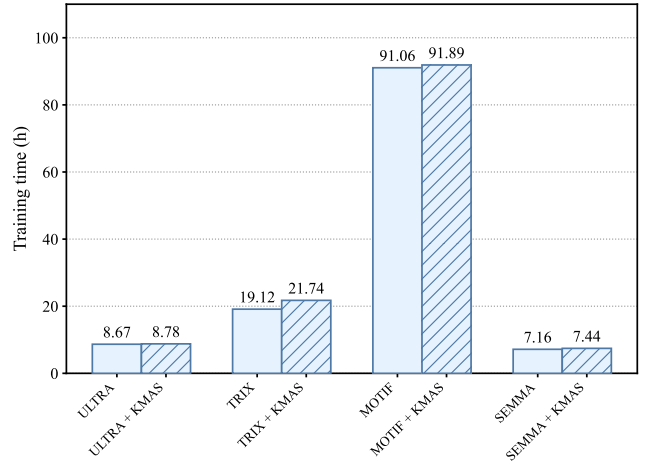


Figure 2: Training time cost comparison of KGfMs (i.e. ULTRA, TRIX, MOTIF, and SEMMA) and these KGfMs using KMAS as the negative sampling method.

original paper [20]. From the experimental results shown in Table 1, it can be seen that our proposed method KMAS can enhance various SOTA KGfMs (i.e., ULTRA, TRIX, MOTIF, and SEMMA) under different settings (i.e., inductive (e, r), inductive (e), and transductive) in terms of MRR and Hits@10, demonstrating the effectiveness of KMAS. We report the detailed results in Appendix B.

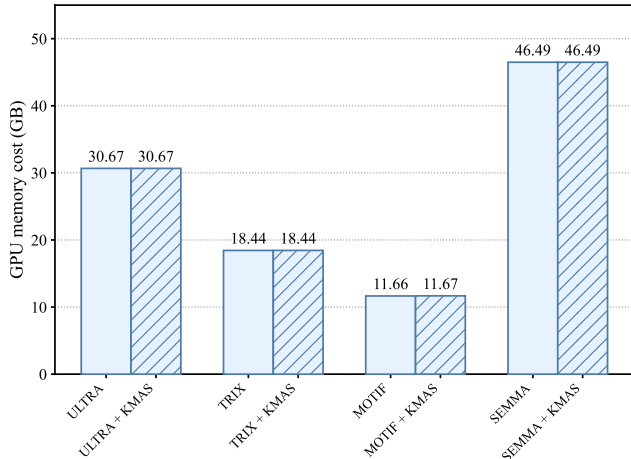
4.3 Efficiency Study

To evaluate the efficiency of KMAS, we test the training time for KMAS combined with different KGfMs on the same training data set (i.e., FB15k-237, WN18RR, and CoDEX-Medium). Since KMAS only performs in the training process, we do not show the inference time. The experimental results plotted in Figure 2 show that KMAS brings a very slight overhead to training time cost across different

¹<https://anonymous.4open.science/r/KGfMs-8C8B>

Table 2: Performance of different variants of KMAS with Ultra/SEMMA as the base KGFM for analysis of the hard negative ratio adjustment strategy under different settings (i.e., inductive (e, r), inductive (e), transductive) over 44 data sets.

Variant	Inductive (e, r) (19 graphs)		Inductive (e) (16 graphs)		Transductive (9 graphs)		Total Avg (44 graphs)	
	MRR	Hits@10	MRR	Hits@10	MRR	Hits@10	MRR	Hits@10
ULTRA + KMAS _{hold}	0.326	0.507	0.431	0.578	0.318	0.469	0.362	0.525
ULTRA + KMAS _{increase}	0.321	0.495	0.427	0.573	0.323	0.472	0.360	0.518
ULTRA + KMAS _{decrease}	0.316	0.497	0.429	0.574	0.328	0.482	0.359	0.522
ULTRA + KMAS	0.326	0.508	0.434	0.584	0.337	0.490	0.367	0.532
SEMMA + KMAS _{hold}	0.331	0.502	0.444	0.585	0.327	0.479	0.371	0.527
SEMMA + KMAS _{increase}	0.328	0.509	0.447	0.589	0.328	0.480	0.371	0.532
SEMMA + KMAS _{decrease}	0.318	0.488	0.447	0.590	0.328	0.478	0.367	0.523
SEMMA + KMAS	0.341	0.517	0.451	0.593	0.336	0.487	0.380	0.539


Figure 3: Memory cost comparison of KGFMs (i.e., ULTRA, TRIX, MOTIF, and SEMMA) and these KGFM using KMAS as the negative sampling method.

KGFM (i.e., ULTRA, TRIX, MOTIF, and SEMMA), demonstrating the efficiency of KMAS. These results are consistent with the time complexity analysis in Section 3.7.

4.4 Memory Cost Study

To evaluate the training memory cost of KMAS, we test the memory cost for KMAS combined with different KGFM on the same training data set (i.e., FB15k-237, WN18RR, and CoDEX-Medium) by tracking the peak memory usage via the `nvidia-smi` command. As plotted in Figure 3, the experimental results show that KMAS does not incur significant additional memory overhead across different KGFM (i.e., ULTRA, TRIX, MOTIF, and SEMMA), demonstrating that KMAS is a memory-efficient method. These results are consistent with the memory complexity analysis in Section 3.7.

4.5 Effect Analysis of Hard Negative Ratio Adjustment

To evaluate the effect of hard negative ratio adjustment strategy, we define 3 different variants of KMAS: (1) KMAS_{hold} (i.e., KMAS using the hard negative ratio α_{max} as α_m for the whole training process); (2) KMAS_{increase} (i.e., KMAS increasing the hard negative ratio α_m from 0 to α_{max} without decreasing); (3) KMAS_{decrease} (i.e., KMAS decreasing α_m from α_{max} to 0 without increasing). From the experimental results shown in Table 2, we can see that KMAS outperforms these three variants (i.e., KMAS_{hold}, KMAS_{increase}, and KMAS_{decrease}) in terms of MRR and Hits@10, whether ULTRA or SEMMA is used as the base KGFM, demonstrating the superiority of our hard negative ratio adjustment strategy.

4.6 Parameter Study

To investigate the robustness of KMAS, we conduct a parameter analysis to understand the impact of q , γ_{peak} , and α_{max} on the performance of SEMMA and KMAS using SEMMA as the base KGFM. Experimental results shown in Figure 4 show that the performance of KMAS using SEMMA as the KGFM outperforms SEMMA itself under different settings (i.e., inductive (e) and transductive) for the different ranges of the three parameters in terms of MRR and Hits@10, demonstrating the robustness of KMAS.

5 Related Work

Three aspects of studies are related to our work: (1) knowledge graph foundation model; (2) negative sampling; (3) curriculum learning. We will introduce them in detail as follows.

Knowledge graph foundation models (KGFM) have emerged as a paradigm for enabling zero-shot reasoning over unseen KGs by learning invariance of the relational structure across diverse KGs. ULTRA [5] pioneered KGFM through the construction of a relation graph \mathcal{G}_R that edges are four fundamental interaction (i.e., $h2h$, $t2h$, $h2t$, $t2t$), enabling zero-shot inference on unseen entities and relations. TRIX [27] enhances ULTRA by using entities as edges bridging relation pairs in its relation graphs and introduces an iterative update schema for joint representation refinement. MOTIF [7] provides a theoretical framework formalizing KGFM based on graph motifs through three steps: LIFT, RELATION ENCODER,

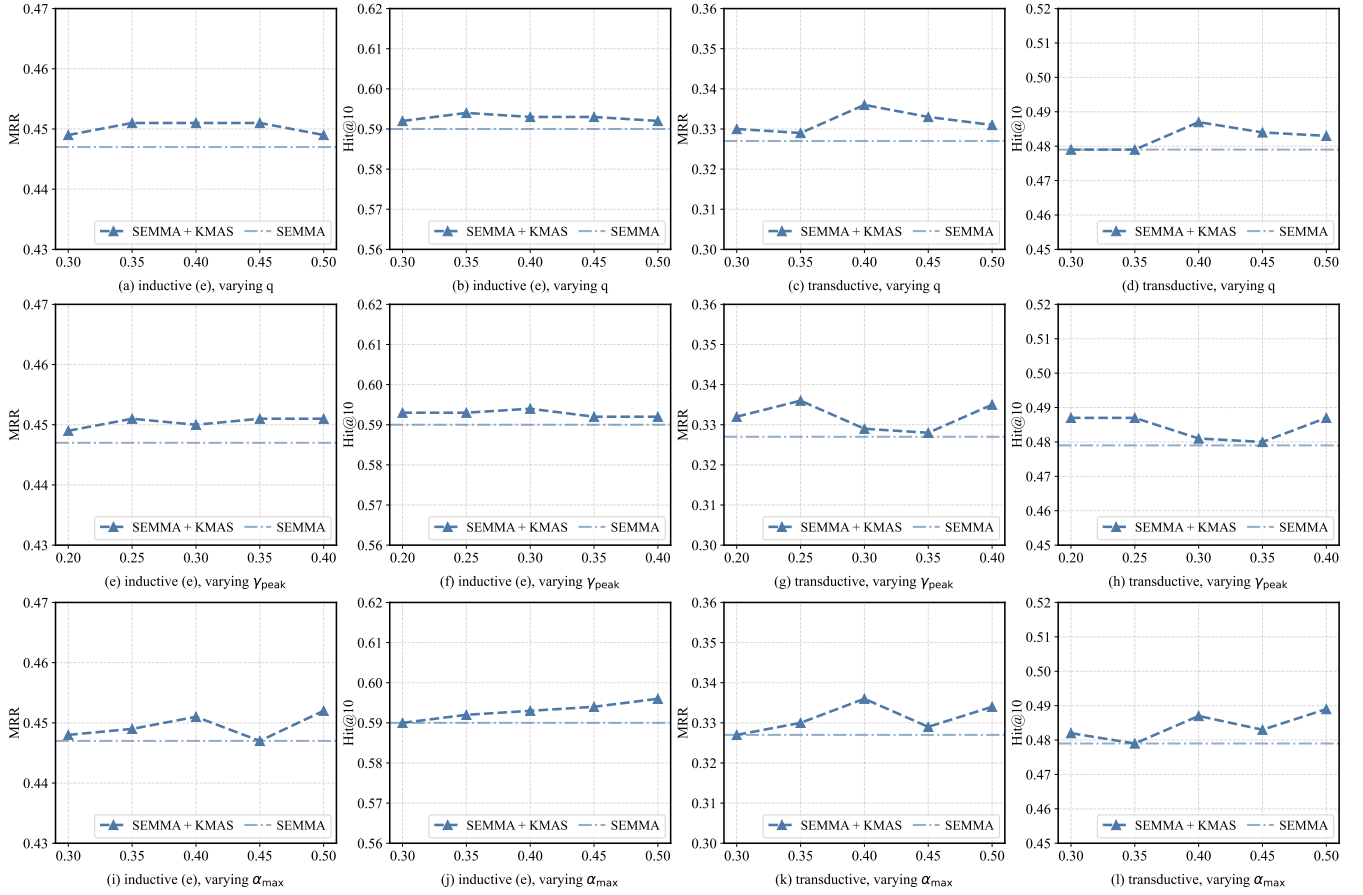


Figure 4: Parameter study results of q , γ_{peak} , and α_{max} .

and ENTITY ENCODER. It reveals ULTRA’s equivalence to binary 2-path motifs and finds that new motifs increase expressiveness only when not covered by core-onto homomorphisms. SEMMA [1] extends KGFMs by combining structural and textual signals. SEMMA obtains textual information via a text relation graph. The outputs from the parallel structural and textual modules are fused via an MLP to generate the final relation embeddings, empowering robust zero-shot link prediction across diverse KGs. SCR [20] improves KGFMs by bridging the gap between structural patterns and node semantic features, while unifying diverse graph tasks into a single reasoning framework. KG-ICL [28] enables universal transfer across diverse KGs by employing a unified tokenizer that maps different entities/relations to the shared tokens based on their relative structural roles and query identity. This mechanism does not rely on the relation graph and processes query-specific prompt graphs, which comprise example facts and their local neighbor and path contexts. Despite significant progress that has been made in KGFMs, the negative sample quality issue is ignored. All KGFMs above rely on corrupting either the head or tail entity of the positive sample to obtain negative samples where negative triples are independent of the invariance of the relation structure. Our work

focuses on boosting KGFMs, which are based on relation graphs via an effective negative sampling method.

The negative sampling method serves as an effective strategy applied in many tasks, such as KG-based recommendation [25], KG completion [21], and KG embedding [8, 10]. In this paper, we dynamically construct hard negative samples for KGFMs through a hybrid negative sampling strategy, enhancing existing KGFMs.

Curriculum learning [2] functions as a sophisticated training paradigm that organizes training examples from easy to hard. Its core idea is applied across various tasks, e.g., complex reasoning over KG [24, 26], KG embedding [6, 18], and joint open knowledge graph canonicalization and linking [16]. Specially, we propose a hard negative ratio adjustment strategy inspired by the trade-off policy, which combines the strategy of “easier first” as curriculum learning and “harder first” as hard example mining [22].

6 Conclusion and Future Work

To enhance existing KGFMs, we propose a simple yet effective adaptive negative sampling method to generate hard negative samples whose ratio is dynamically adjusted to train KGFMs. KMAS is flexible to adapt to many KGFMs. Extensive experiments are conducted on 44 data sets. Experimental results have demonstrated that KMAS

can improve the performance of many SOTA KGFMs without requiring excessive additional time or memory consumption. In the future, we will evaluate the performance of KMAS on more KGFMs and data sets.

References

- [1] Arvindh Arun, Sumit Kumar, Mojtaba Nayyeri, Bo Xiong, Ponnurangam Kumaraguru, Antonio Vergari, and Steffen Staab. 2025. SEMMA: A Semantic Aware Knowledge Graph Foundation Model. In *EMNLP*. 31825–31848.
- [2] Yoshua Bengio, Jérôme Louradour, Ronan Collobert, and Jason Weston. 2009. Curriculum learning. In *ICML*. 41–48.
- [3] Antoine Bordes, Nicolas Usunier, Alberto Garcia-Duran, Jason Weston, and Oksana Yakhnenko. 2013. Translating Embeddings for Modeling Multi-relational Data. In *NIPS*. 2787–2795.
- [4] Tim Dettmers, Pasquale Minervini, Pontus Stenetorp, and Sebastian Riedel. 2018. Convolutional 2d knowledge graph embeddings. In *AAAI*. 1811–1818.
- [5] Mikhail Galkin, Xinyu Yuan, Hesham Mostafa, Jian Tang, and Zhaocheng Zhu. 2024. Towards Foundation Models for Knowledge Graph Reasoning. In *ICLR*.
- [6] Shu Guo, Quan Wang, Lihong Wang, Bin Wang, and Li Guo. 2018. Knowledge Graph Embedding with Iterative Guidance from Soft Rules. In *AAAI*. 4816–4823.
- [7] Xingyue Huang, Pablo Barceló, Michael M. Bronstein, İsmail İlkan Ceylan, Mikhail Galkin, Juan L. Reutter, and Miguel Romero Orth. 2025. How Expressive are Knowledge Graph Foundation Models?. In *ICML*.
- [8] Vibhor Kanojia, Hideyuki Maeda, Riku Togashi, and Sumio Fujita. 2017. Enhancing Knowledge Graph Embedding with Probabilistic Negative Sampling. In *WWW*. 801–802.
- [9] Jaemin Lee, Chanyoung Chung, and Joyce Jiyoun Whang. 2023. INGRAM: inductive knowledge graph embedding via relation graphs. In *ICML*.
- [10] Zhenzhou Lin, Zishuo Zhao, Jingyou Xie, and Ying Shen. 2023. Hierarchical Type Enhanced Negative Sampling for Knowledge Graph Embedding. In *SIGIR*. 2047–2051.
- [11] Shuwen Liu, Bernardo Cuenca Grau, Ian Horrocks, and Egor V. Kostylev. 2021. INDIGO: GNN-Based Inductive Knowledge Graph Completion Using Pair-Wise Encoding. In *NIPS*. 2034–2045.
- [12] Shirui Pan, Linhao Luo, Yufei Wang, Chen Chen, Jiapu Wang, and Xindong Wu. 2024. Unifying Large Language Models and Knowledge Graphs: A Roadmap. *IEEE Transactions on Knowledge and Data Engineering* 36, 7 (2024), 3580–3599.
- [13] Andrea Rossi, Denilson Barbosa, Donatella Firmani, Antonio Matinata, and Paolo Merialdo. 2021. Knowledge Graph Embedding for Link Prediction: A Comparative Analysis. *ACM Transactions on Knowledge Discovery from Data* 15, 2 (2021).
- [14] Andrea Rossi, Donatella Firmani, Paolo Merialdo, and Tommaso Teofili. 2022. Explaining Link Prediction Systems based on Knowledge Graph Embeddings. In *SIGMOD*. 2062–2075.
- [15] Tara Safavi and Danai Koutra. 2020. CoDEX: A Comprehensive Knowledge Graph Completion Benchmark. In *EMNLP*. 8328–8350.
- [16] Wei Shen, Binhan Yang, and Yinan Liu. 2024. Jointly Canonicalizing and Linking Open Knowledge Base via Unified Embedding Learning. In *WWW*. 2304–2314.
- [17] Zhiqing Sun, Zhi-Hong Deng, Jian-Yun Nie, and Jian Tang. 2019. RotatE: Knowledge Graph Embedding by Relational Rotation in Complex Space. In *ICLR*.
- [18] Zequn Sun, Wei Hu, Qingheng Zhang, and Yuzhong Qu. 2018. Bootstrapping Entity Alignment with Knowledge Graph Embedding. In *IJCAI*. 4396–4402.
- [19] Kristina Toutanova and Danqi Chen. 2015. Observed versus latent features for knowledge base and text inference. In *Proceedings of the 3rd workshop on continuous vector space models and their compositionality*. 57–66.
- [20] Kai Wang, Siqiang Luo, Caihua Shan, and Yifei Shen. 2025. Towards graph foundation models: Training on knowledge graphs enables transferability to general graphs. In *NIPS*.
- [21] Liang Wang, Wei Zhao, Zhuoyu Wei, and Jingming Liu. 2022. SimKGC: Simple Contrastive Knowledge Graph Completion with Pre-trained Language Models. In *ACL*. 4281–4294.
- [22] Xin Wang, Yudong Chen, and Wenwu Zhu. 2021. A Survey on Curriculum Learning. *IEEE Transactions on Pattern Analysis and Machine Intelligence* 14, 8 (2021), 1–20.
- [23] Xiang Wang, Xiangnan He, Yixin Cao, Meng Liu, and Tat-Seng Chua. 2019. KGAT: Knowledge Graph Attention Network for Recommendation. In *SIGKDD*. 950–958.
- [24] Tianle Xia, Liang Ding, Guojia Wan, Yibing Zhan, Bo Du, and Dacheng Tao. 2025. Improving Complex Reasoning over Knowledge Graph with Logic-Aware Curriculum Tuning. In *AAAI*. 12881–12889.
- [25] Yuhao Yang, Chao Huang, Lianghao Xia, and Chenliang Li. 2022. Knowledge Graph Contrastive Learning for Recommendation. In *SIGIR*. 1434–1443.
- [26] Wen Zhang, Bibek Paudel, Liang Wang, Jiaoyan Chen, Hai Zhu, Wei Zhang, Abraham Bernstein, and Huajun Chen. 2019. Iteratively Learning Embeddings and Rules for Knowledge Graph Reasoning. In *WWW*. 2366–2377.
- [27] Yucheng Zhang, Beatrice Bevilacqua, Mikhail Galkin, and Bruno Ribeiro. 2024. TRIX: A More Expressive Model for Zero-shot Domain Transfer in Knowledge Graphs. In *LoG*.
- [28] Ruilin Zhao, Feng Zhao, Long Wang, Xianzhi Wang, and Guandong Xu. 2024. KG-CoT: Chain-of-thought prompting of large language models over knowledge graphs for knowledge-aware question answering. In *IJCAI*. 6642–6650.
- [29] Zhaocheng Zhu, Zuobai Zhang, Louis-Pascal Xhonneux, and Jian Tang. 2021. Neural bellman-ford networks: A general graph neural network framework for link prediction. In *NIPS*. 29476–29490.

Appendix

A Data Sets

We train KGFMs on 3 KGs and inference on 44 data sets. The statistics of 3 KGs for training in Table 3 and 9 data sets of the transductive setting for inference are shown in Table 4. The statistics of 16 data sets of the partially inductive setting (i.e., inductive (e)) for inference are shown in Table 5. The statistics of 19 data sets of the fully inductive setting (i.e., inductive (e, r)) for inference are shown in Table 6.

B Detailed Results

We show detailed results of four KGFMs (i.e., ULTRA, TRIX, MOTIF, and SEMMA) and these KGFMs enhanced by KMAS over 44 data sets in Table 7, Table 8, Table 9, and Table 10 corresponding to the results in Table 1.

Table 3: 3 KGs for training. E denotes the number of entities. R denotes the number of relations. Train, Valid, and Test denote the number of triples for training, validation, and test in the corresponding data set. Task denotes the prediction task. h/t means the task of predicting both head entities and tail entities.

Data set	E	R	Train	Valid	Test	Task
CoDEXMedium	17050	51	185584	10310	10311	h/t
FB15k237	14541	237	272115	17535	20466	h/t
WN18RR	40943	11	86835	3034	3134	h/t

Table 4: 9 data sets of the transductive setting for inference. Task denotes the prediction task. h/t means the task of predicting both head entities and tail entities, tails means the task of predicting the tail entity.

Data set	E	R	Train	Valid	Test	Task
CoDEXSmall	2034	42	32888	1827	1828	h/t
CoDEXLarge	77113	69	511359	30622	30622	h/t
NELL995	74536	200	149678	543	2818	h/t
WDSinger	10282	135	16142	2163	2203	h/t
NELL23k	22925	200	25445	4961	4952	h/t
FB15k237_10	11512	237	27211	15624	18150	tails
FB15k237_20	13166	237	54423	16963	19776	tails
FB15k237_50	14149	237	136057	17449	20324	tails
Hetionet	45158	24	2025177	112510	112510	h/t

Table 5: 16 data sets of the partially inductive setting. T denotes the number of triples in their corresponding graph. Valid and Test denote the triples that need to be predicted in the validation and test data sets in their corresponding graph. We predict both head entities and tail entities for these data sets.

<i>Data set</i>	<i>R</i>	<i>Train Graph</i>		<i>Validation Graph</i>			<i>Test Graph</i>		
		<i>E</i>	<i>T</i>	<i>E</i>	<i>T</i>	<i>Valid</i>	<i>E</i>	<i>T</i>	<i>Test</i>
WN18RRInductive:v1	9	2746	5410	2746	5410	630	922	1618	373
WN18RRInductive:v2	10	6954	15262	6954	15262	1838	2757	4011	852
WN18RRInductive:v3	11	12078	25901	12078	25901	3097	5084	6327	1143
WN18RRInductive:v4	9	3861	7940	3861	7940	934	7084	12334	2823
FB15k237Inductive:v1	180	1594	4245	1594	4245	489	1093	1993	411
FB15k237Inductive:v2	200	2608	9739	2608	9739	1166	1660	4145	947
FB15k237Inductive:v3	215	3668	17986	3668	17986	2194	2501	7406	1731
FB15k237Inductive:v4	219	4707	27203	4707	27203	3352	3051	11714	2840
NELLInductive:v2	88	2564	8219	2564	8219	922	2086	4586	935
NELLInductive:v3	142	4647	16393	4647	16393	1851	3566	8048	1620
NELLInductive:v4	76	2092	7546	2092	7546	876	2795	7073	1447
ILPC2022:small	48	10230	78616	6653	20960	2908	6653	20960	2902
ILPC2022:large	65	46626	202446	29246	77044	10179	29246	77044	10184
HM 3k	11	32118	71097	32250	71097	1201	19218	38285	1349
HM 5k	11	28601	57601	28744	57601	900	23792	48425	2124
IndigoBM	229	12721	121601	12797	121601	14121	14775	250195	14904

Table 6: 19 data sets of the fully inductive setting. We predict both head entities and tail entities for these data sets.

<i>Data set</i>	<i>Train Graph</i>			<i>Validation Graph</i>				<i>Test Graph</i>			
	<i>E</i>	<i>R</i>	<i>T</i>	<i>E</i>	<i>R</i>	<i>T</i>	<i>Valid</i>	<i>E</i>	<i>R</i>	<i>T</i>	<i>Test</i>
FBIngram:100	4659	134	62809	2624	77	6987	2329	2624	77	6987	2329
FBIngram:75	4659	134	62809	2792	186	9316	3106	2792	186	9316	3106
FBIngram:50	5190	153	85375	4445	205	11636	3879	4445	205	11636	3879
FBIngram:25	5190	163	91571	4097	216	17147	5716	4097	216	17147	5716
WKIngram:100	9784	67	49875	12136	37	13487	4496	12136	37	13487	4496
WKIngram:75	6853	52	28741	2722	65	3430	1143	2722	65	3430	1144
WKIngram:50	12022	72	82481	9328	93	9672	3224	9328	93	9672	3225
WKIngram:25	12659	47	41873	3228	74	3391	1130	3228	74	3391	1131
NLIngram:75	2607	96	11058	1578	116	1818	606	1578	116	1818	607
NLIngram:50	4396	106	17578	2335	119	2576	859	2335	119	2576	859
NLIngram:25	4396	106	17578	2146	120	2230	743	2146	120	2230	744
MT1 tax	10000	10	17178	10000	10	17178	1908	10000	9	16526	1834
MT2 org	10000	10	23233	10000	10	23233	2581	10000	11	21976	2441
MT2 sci	10000	16	16471	10000	16	16471	1830	10000	16	14852	1650
MT3 art	10000	45	27262	10000	45	27262	3026	10000	45	28023	3113
MT3 infra	10000	24	21990	10000	24	21990	2443	10000	27	21646	2405
MT4 sci	10000	42	12576	10000	42	12576	1397	10000	42	12516	1388
Metafam	1316	28	13821	1316	28	13821	590	656	28	7257	184
FBNELL	4636	100	10275	4636	100	10275	1055	4752	183	10685	597

Table 7: Detail results of the KGFM ULTRA and ULTRA using KMAS as the negative sampling method.

<i>Data set</i>	ULTRA		ULTRA + KMAS	
	<i>MRR</i>	<i>Hits@10</i>	<i>MRR</i>	<i>Hits@10</i>
<i>Transductive</i>				
CoDExSmall	0.473	0.670	0.476	0.670
CoDExLarge	0.340	0.474	0.339	0.471
NELL995	0.472	0.594	0.476	0.605
WDSinger	0.351	0.480	0.387	0.504
NELL23k	0.235	0.402	0.235	0.408
FB15k237_10	0.235	0.380	0.240	0.391
FB15k237_20	0.265	0.423	0.268	0.431
FB15k237_50	0.323	0.519	0.324	0.523
Hetionet	0.284	0.406	0.284	0.406
<i>Inductive (e)</i>				
WN18RRInductive:v1	0.658	0.776	0.652	0.794
WN18RRInductive:v2	0.658	0.772	0.657	0.771
WN18RRInductive:v3	0.373	0.496	0.383	0.510
WN18RRInductive:v4	0.605	0.714	0.605	0.716
FB15k237Inductive:v1	0.484	0.645	0.495	0.647
FB15k237Inductive:v2	0.486	0.684	0.491	0.693
FB15k237Inductive:v3	0.483	0.650	0.485	0.646
FB15k237Inductive:v4	0.483	0.672	0.482	0.674
NELLInductive:v2	0.499	0.696	0.536	0.720
NELLInductive:v3	0.521	0.706	0.530	0.713
NELLInductive:v4	0.477	0.711	0.495	0.729
ILPC2022:small	0.292	0.444	0.293	0.452
ILPC2022:large	0.283	0.420	0.295	0.424
HM:3k	0.061	0.107	0.054	0.109
HM:5k	0.054	0.102	0.050	0.099
HM:indigo	0.440	0.649	0.436	0.646
<i>Inductive (e, r)</i>				
FBIngram:100	0.439	0.627	0.439	0.632
FBIngram:75	0.394	0.595	0.400	0.599
FBIngram:50	0.329	0.532	0.333	0.541
FBIngram:25	0.387	0.634	0.392	0.639
WKIngram:100	0.178	0.291	0.184	0.302
WKIngram:75	0.373	0.520	0.379	0.536
WKIngram:50	0.143	0.295	0.151	0.308
WKIngram:25	0.286	0.498	0.297	0.512
NLIngram:75	0.347	0.513	0.325	0.502
NLIngram:50	0.382	0.559	0.376	0.532
NLIngram:25	0.381	0.556	0.371	0.558
WikiTopicsMT1:tax	0.223	0.308	0.233	0.320
WikiTopicsMT2:org	0.088	0.153	0.090	0.153
WikiTopicsMT2:sci	0.236	0.390	0.296	0.428
WikiTopicsMT3:art	0.244	0.409	0.261	0.422
WikiTopicsMT3:infra	0.640	0.779	0.636	0.780
WikiTopicsMT4:sci	0.298	0.455	0.299	0.460
Metafam	0.177	0.726	0.267	0.788
FBNEL	0.479	0.646	0.482	0.646

Table 8: Detail results of the KGFM TRIX and TRIX using KMAS as the negative sampling method.

<i>Data set</i>	TRIX		TRIX + KMAS	
	<i>MRR</i>	<i>Hits@10</i>	<i>MRR</i>	<i>Hits@10</i>
<i>Transductive</i>				
CoDExSmall	0.391	0.638	0.390	0.637
CoDExLarge	0.317	0.446	0.310	0.446
NELL995	0.432	0.588	0.472	0.612
WDSinger	0.370	0.495	0.379	0.501
NELL23k	0.228	0.388	0.224	0.380
FB15k237_10	0.233	0.379	0.223	0.369
FB15k237_20	0.259	0.415	0.258	0.416
FB15k237_50	0.314	0.506	0.312	0.509
Hetionet	0.191	0.352	0.195	0.366
<i>Inductive (e)</i>				
WN18RRInductive:v1	0.644	0.798	0.687	0.804
WN18RRInductive:v2	0.646	0.787	0.684	0.785
WN18RRInductive:v3	0.445	0.569	0.446	0.569
WN18RRInductive:v4	0.588	0.710	0.647	0.727
FB15k237Inductive:v1	0.484	0.646	0.489	0.651
FB15k237Inductive:v2	0.499	0.711	0.516	0.709
FB15k237Inductive:v3	0.486	0.658	0.492	0.656
FB15k237Inductive:v4	0.476	0.683	0.485	0.676
NELLInductive:v2	0.563	0.769	0.558	0.761
NELLInductive:v3	0.567	0.757	0.563	0.749
NELLInductive:v4	0.538	0.764	0.533	0.765
ILPC2022:small	0.303	0.455	0.303	0.453
ILPC2022:large	0.305	0.430	0.300	0.427
HM:3k	0.072	0.126	0.066	0.122
HM:5k	0.066	0.109	0.063	0.110
HM:indigo	0.432	0.640	0.433	0.644
<i>Inductive (e, r)</i>				
FBIngram:100	0.441	0.640	0.445	0.642
FBIngram:75	0.397	0.606	0.392	0.595
FBIngram:50	0.338	0.545	0.327	0.540
FBIngram:25	0.391	0.647	0.391	0.644
WKIngram:100	0.184	0.294	0.184	0.294
WKIngram:75	0.384	0.524	0.376	0.519
WKIngram:50	0.170	0.305	0.160	0.291
WKIngram:25	0.299	0.485	0.296	0.466
NLIngram:75	0.348	0.521	0.347	0.526
NLIngram:50	0.391	0.582	0.382	0.551
NLIngram:25	0.389	0.589	0.368	0.562
WikiTopicsMT1:tax	0.270	0.433	0.276	0.445
WikiTopicsMT2:org	0.096	0.153	0.094	0.151
WikiTopicsMT2:sci	0.279	0.433	0.328	0.466
WikiTopicsMT3:art	0.296	0.450	0.296	0.454
WikiTopicsMT3:infra	0.638	0.781	0.661	0.793
WikiTopicsMT4:sci	0.294	0.451	0.292	0.448
Metafam	0.316	0.823	0.377	0.880
FBNEL	0.491	0.681	0.475	0.670

Table 9: Detail results of the KGFM MOTIF and MOTIF using KMAS as the negative sampling method.

<i>Data set</i>	MOTIF		MOTIF + KMAS	
	<i>MRR</i>	<i>Hits@10</i>	<i>MRR</i>	<i>Hits@10</i>
<i>Transductive</i>				
CoDExSmall	0.472	0.668	0.470	0.667
CoDExLarge	0.331	0.462	0.340	0.471
NELL995	0.440	0.596	0.468	0.616
WDSinger	0.372	0.485	0.379	0.498
NELL23k	0.220	0.374	0.223	0.389
FB15k237_10	0.244	0.390	0.244	0.390
FB15k237_20	0.263	0.421	0.266	0.424
FB15k237_50	0.313	0.510	0.318	0.514
Hetionet	0.264	0.386	0.284	0.406
<i>Inductive (e)</i>				
WN18RRInductive:v1	0.663	0.777	0.686	0.787
WN18RRInductive:v2	0.663	0.769	0.658	0.773
WN18RRInductive:v3	0.430	0.565	0.425	0.547
WN18RRInductive:v4	0.629	0.705	0.630	0.709
FB15k237Inductive:v1	0.485	0.669	0.484	0.681
FB15k237Inductive:v2	0.494	0.719	0.494	0.715
FB15k237Inductive:v3	0.486	0.664	0.471	0.663
FB15k237Inductive:v4	0.480	0.673	0.478	0.668
NELLInductive:v2	0.527	0.724	0.532	0.742
NELLInductive:v3	0.504	0.678	0.521	0.696
NELLInductive:v4	0.475	0.685	0.471	0.731
ILPC2022:small	0.286	0.439	0.292	0.445
ILPC2022:large	0.274	0.416	0.269	0.413
HM:3k	0.059	0.100	0.100	0.107
HM:5k	0.050	0.087	0.056	0.099
HM:indigo	0.428	0.638	0.431	0.640
<i>Inductive (e, r)</i>				
FBIngram:100	0.437	0.629	0.428	0.625
FBIngram:75	0.394	0.601	0.389	0.601
FBIngram:50	0.332	0.528	0.336	0.542
FBIngram:25	0.380	0.626	0.388	0.637
WKIngram:100	0.174	0.294	0.164	0.288
WKIngram:75	0.366	0.531	0.368	0.518
WKIngram:50	0.165	0.318	0.165	0.311
WKIngram:25	0.321	0.514	0.309	0.506
NLIngram:75	0.324	0.488	0.327	0.498
NLIngram:50	0.380	0.527	0.374	0.538
NLIngram:25	0.326	0.454	0.336	0.519
WikiTopicsMT1:tax	0.244	0.342	0.258	0.408
WikiTopicsMT2:org	0.094	0.153	0.090	0.153
WikiTopicsMT2:sci	0.275	0.422	0.266	0.428
WikiTopicsMT3:art	0.259	0.409	0.263	0.412
WikiTopicsMT3:infra	0.620	0.764	0.638	0.772
WikiTopicsMT4:sci	0.287	0.462	0.276	0.429
Metafam	0.417	0.764	0.488	0.807
FBNELL	0.463	0.633	0.468	0.651

Table 10: Detail results of the KGFM SEMMA and SEMMA using KMAS as the negative sampling method.

<i>Data set</i>	SEMMA		SEMMA + KMAS	
	<i>MRR</i>	<i>Hits@10</i>	<i>MRR</i>	<i>Hits@10</i>
<i>Transductive</i>				
CoDExSmall	0.489	0.676	0.484	0.679
CoDExLarge	0.346	0.479	0.337	0.473
NELL995	0.416	0.546	0.468	0.604
WDSinger	0.390	0.503	0.395	0.502
NELL23k	0.241	0.413	0.238	0.412
FB15k237_10	0.233	0.385	0.241	0.385
FB15k237_20	0.262	0.430	0.266	0.427
FB15k237_50	0.326	0.524	0.329	0.525
Hetionet	0.237	0.356	0.264	0.375
<i>Inductive (e)</i>				
WN18RRInductive:v1	0.709	0.806	0.702	0.808
WN18RRInductive:v2	0.695	0.795	0.702	0.800
WN18RRInductive:v3	0.445	0.591	0.445	0.592
WN18RRInductive:v4	0.658	0.739	0.654	0.730
FB15k237Inductive:v1	0.495	0.647	0.504	0.656
FB15k237Inductive:v2	0.513	0.696	0.508	0.695
FB15k237Inductive:v3	0.496	0.654	0.504	0.658
FB15k237Inductive:v4	0.498	0.674	0.496	0.681
NELLInductive:v2	0.526	0.711	0.531	0.728
NELLInductive:v3	0.497	0.691	0.525	0.715
NELLInductive:v4	0.480	0.726	0.492	0.727
ILPC2022:small	0.303	0.455	0.301	0.452
ILPC2022:large	0.303	0.426	0.304	0.426
HM:3k	0.053	0.084	0.057	0.094
HM:5k	0.051	0.096	0.051	0.086
HM:indigo	0.430	0.643	0.433	0.644
<i>Inductive (e, r)</i>				
FBIngram:100	0.454	0.643	0.452	0.639
FBIngram:75	0.403	0.598	0.409	0.607
FBIngram:50	0.342	0.548	0.341	0.546
FBIngram:25	0.399	0.644	0.400	0.649
WKIngram:100	0.185	0.295	0.187	0.303
WKIngram:75	0.382	0.526	0.381	0.515
WKIngram:50	0.173	0.319	0.175	0.322
WKIngram:25	0.312	0.481	0.308	0.489
NLIngram:75	0.349	0.523	0.386	0.528
NLIngram:50	0.394	0.573	0.386	0.550
NLIngram:25	0.382	0.532	0.388	0.573
WikiTopicsMT1:tax	0.233	0.310	0.252	0.398
WikiTopicsMT2:org	0.095	0.158	0.095	0.159
WikiTopicsMT2:sci	0.237	0.340	0.258	0.398
WikiTopicsMT3:art	0.270	0.416	0.277	0.423
WikiTopicsMT3:infra	0.634	0.769	0.643	0.778
WikiTopicsMT4:sci	0.283	0.448	0.278	0.447
Metafam	0.300	0.769	0.408	0.856
FBNELL	0.464	0.644	0.485	0.647